Multimode Ultrasound Features in Skeletal Muscle Lymphoma

A Retrospective Observational Study

Yang Sun, MD, Li Zhang, MM, Jing Su, MD, Iryna Vyacheslavovna Nazarenko, MD, Dzmitry Ivanovich Haurylenka, MD, Ligang Cui, MD, Wen Chen, MD

Received February 13, 2025, from the Department of Ultrasound, Peking University Third Hospital, Beijing, China (Y.S., L.C., W.C.); Department of Ultrasound, Beijing Chaoyang Hospital, Capital Medical University, Beijing, China (L.Z.); Department of Pathology, School of Basic Medical Science, Peking University Health Science Center, Beijing, China (J.S.); Department of Radiation Diagnostics, Medical Diagnostic Faculty of Gomel State Medical University, Gomel, Belarus (I.V.N.); and Department of the Functional Diagnostics and Radionuclide Methods, Republican Scientific and Practical Centre for Radiation Medicine and Human Ecology, Gomel, Belarus (D.I.H.). Manuscript accepted for publication July 21, 2025.

This study has received funding from the National Natural Science Foundation of China (82102071). The authors declare that they have no competing interests.

Yang Sun and Li Zhang contributed equally to this work and should be considered joint first author.

Address correspondence to Ligang Cui, Department of Ultrasound, Peking University Third Hospital, 49 North Garden Road, Haidian District, Beijing 100191, China.

E-mail: cuiligang_bysy@126.com

Wen Chen, Department of Ultrasound, Peking University Third Hospital, 49 North Garden Road, Haidian District, Beijing 100191, China.

E-mail: wendy7989@sina.com

Abbreviations

CEUS, contrast-enhanced ultrasound; HE, hematoxylin and eosin; MRI, magnetic resonance imaging; PET-CT, positron emission tomography–computed tomography; SD, standard deviation

doi:10.1002/jum.70018

Objectives—This study aimed to evaluate the ultrasound findings in skeletal muscle lymphoma and investigate the correlations between ultrasound findings and histopathological characteristics.

Methods—Ultrasonographic images with skeletal muscle lymphoma obtained between June 2014 and June 2024 were retrospectively reviewed. The ultrasonographic examinations comprised gray-scale (n = 35), color-Doppler (n = 35), contrast-enhanced (n = 5), and elastography imaging (n = 5). Biopsy samples underwent histopathological analysis to identify the histopathologic basis of the typical ultrasound features. Kappa statistics were used to assess the consistency between ultrasound findings and histopathological features.

Results—The study comprised 35 patients (mean age, 63 years ±15 [standard deviation], 17 men). In gray-scale sonography, 35 lesions (100%) appeared as hypoechoic areas in the muscle with poorly defined margins. Residual myofiber-like echoes were observed in 25 (71.4%) lesions, and a "cobblestone" appearance was noted in 18 (51.4%). In color-Doppler sonography, 10 (28.6%) patients had intact transverse vessels perpendicular to the long axis of the muscle. In contrast-enhanced sonography, 4 out of 5 (80%) lesions showed synchronous high enhancement. Four out of 5 (80%) lesions exhibited high stiffness on elastography imaging. Myofiber-like echoes (κ: 0.800, $P < 0.001$) and the "cobblestone" appearance (κ: 0.521, $P < .017$) are consistent with myofibers in pathology.

Conclusion—Skeletal muscle lymphoma demonstrates specific features on multimodal ultrasound.

Key Words—diagnosis; elasticity imaging techniques; lymphoma; sonography

Lymphoma is a complex disease that primarily targets the lymph nodes but can also affect other body systems, with extranodal lymphoma commonly found in the gastrointestinal tract, lungs, and nervous system.[1] However, lymphoma rarely invades skeletal muscle, occurring in only about 1.5% of non-Hodgkin lymphoma cases and a mere 0.3% of Hodgkin lymphoma cases.[2] Such skeletal muscle lymphomas are classified according to their onset as primary lymphomas, hematogenous metastases, and direct invasion.[3] Patients with skeletal muscle lymphoma often present with subtle symptoms, prompting them to seek medical attention due to palpable masses or visible muscle enlargement on the body surface.[4]

If the attending physician has inadequate knowledge of muscle lymphoma, masses within muscles are prone to being misdiagnosed as sarcomas, leading to potentially unnecessary surgical interventions. Ultrasound serves as the initial diagnostic tool for

such patients and plays a crucial role in their management. Therefore, identifying the imaging features of muscle lymphoma may aid in effectively triaging patients, choosing the right time for biopsy, and avoiding unnecessary surgeries. However, because of the rarity of skeletal muscle lymphomas, there is a scarcity of reports documenting their ultrasound manifestations, and a notable lack of comprehensive analyses of their ultrasound features in large patient groups.

The present study aimed to evaluate the ultrasound findings in skeletal muscle lymphoma, explore the underlying pathological mechanisms of these features, and investigate the correlations between ultrasound findings and histopathological characteristics.

Materials and Methods

Patients

This study was approved by the Ethics Committee of our hospital (approval no. M2023510). A retrospective analysis was conducted of ultrasound images and histological sections from patients examined between June 2014 and June 2024. Patients included in the study needed to meet the following criteria: 1) a diagnosis of lymphoma through either biopsy or surgical resection; if the biopsy was from skeletal muscle, it was pathologically confirmed as skeletal muscle lymphoma, without the need for additional diagnostic tests; if the biopsy was from non-skeletal muscle tissue, positron emission tomography–computed tomography (PET-CT) must have shown metabolically active lesions in skeletal muscle that had substantially reduced or disappeared after chemotherapy, with a final clinical diagnosis of skeletal muscle lymphoma; detailed clinical records of the chief complaints, present illness, medical history, general condition, physical examination reports, and past diagnostic tests; 2) gray-scale ultrasound images clearly showing the number, overall shape, margins, internal echoes, and surrounding soft tissue of the skeletal muscle lymphoma lesions; 3) availability of a color-Doppler sonogram of the lesion area. The exclusion criteria were: 1) missing or unclear histopathological slides that could not be diagnosed as skeletal muscle lymphoma; 2) incomplete clinical information preventing a diagnosis of skeletal muscle lymphoma; 3) lesions not clearly visualized or incompletely depicted on gray-scale ultrasound images; 4) elastic sonogram showing only the lesion area, without stiffness data for the surrounding normal muscle tissue; 5) contrast-enhanced ultrasound (CEUS) videos showing only the lesion area, without information about the surrounding normal muscle tissue.

Clinical Characteristics

In this study, the clinical information to be collected mainly includes the site of onset, clinical manifestations, general condition, and involvement of other tissues or organs. This information was recorded by the patient's attending hematologist in the medical record database at the time of admission.

Pathological Analysis

All patients underwent ultrasound-guided in-plane percutaneous biopsy. Samples were fixed in a 10% neutral formaldehyde solution for 24 hours at 18°C, embedded in paraffin, and cut into 3-μm-thick sections. These sections were then stained with routine hematoxylin and eosin (HE) for 2 hours at 18°C. Subsequently, the sections were dehydrated with 95% alcohol (repeated 4 times for 5 minutes each time) and xylene (repeated twice for 5 minutes each time), before being sealed with neutral balsam. Sections from all patients underwent histological examination to confirm the diagnosis and subtype of lymphoma. HE staining and immunohistochemical staining were performed in all cases to confirm the diagnosis of lymphoma. Some cases had additional molecular tests performed, including IgG rearrangement, T cell receptor rearrangement, detection of Epstein–Barr virus-encoded RNA, and fluorescence in situ hybridization analysis.

Ultrasound Image Review

Three physicians (each with over 10 years of experience in ultrasound) independently reviewed the retained images. During the image review, the physicians were blinded to the histopathological results. When 2 physicians agreed on the findings, their consensus was adopted. In cases of disagreement, a third physician was asked to assess the images. The final result was based on the outcome with the highest agreement rate among the 3 physicians.

All gray-scale ultrasound sonograms were acquired using linear (4–15 MHz) or convex (1–7 MHz) transducers. The ultrasound systems used to capture the imaging reviewed in this study were the Logic E9 (GE, Waukesha, USA), Acuson S3000 (Siemens, Mountain View, CA, USA), RS85 (Samsung, Seoul, South Korea), Aplio i900 (Canon Medical Systems, Otawara, Japan), VISION (Hitachi Medical Corporation; Tokyo, Japan), Resona 7 (Mindray, Shenzhen, China), and Supersonic (Aixplorer, Aix-en-Provence, France) systems. The pulse repetition frequency for color-Doppler assessment of the masses was recorded using linear transducers (0.2–2.4 kHz) or convex transducers (0.5–4.2 kHz). Elastography imaging consisted of strain elastography or shear wave elastography. Contrast-enhanced imaging was performed using the ultrasound contrast agent SonoVue® (Bracco S.p.A., Milan, Italy), which consists of sulfur hexafluoride-filled microbubbles enveloped by a phospholipid shell.

Gray-Scale Ultrasound

In gray-scale images, the following findings were analyzed: single or multiple, size of the lesion, relationship of the lesion to the long axis of the affected muscle, continuity of the epimysium of the affected muscle, presence of thickening of the overlying skin and subcutaneous fat, presence of calcification, echogenicity of the lesion, and internal architecture of the lesion.

Upon examination of the internal architecture of the lesion, the following features were observed: 1) residual myofiber-like echoes defined as parallel linear hyperechoic areas within a hypoechoic zone, continuing with the surrounding normal muscle fibers, which may be interrupted, blurred, or partially absent (Figure 1); 2) "cobblestone" appearance characterized by the intertwining of hyperechoic and hypoechoic areas, segmenting the hyperechoic zone into unevenly sized blocks (Figure 1); 3) mass-like appearance defined as a hypoechoic mass with no visible myofiber-like echoes or "cobblestone" appearance.

Color-Doppler Ultrasound

The sonogram was evaluated for the presence of transverse vessels, defined as blood flow signals that were perpendicular to the long axis of the muscle. The color-Doppler flow images were categorized as follows: "rich blood flow signals" defined as tree-like (branching) blood flow signals; "minimal blood flow signals" defined as short, rod-like or dot-like blood flow signals; "no blood flow signals" defined as the absence of blood flow signals within the region of interest.

Contrast-Enhanced Ultrasound

The CEUS images were assessed to determine whether the lesion demonstrated homogeneous enhancement, inhomogeneous enhancement, or no enhancement.

Elastography

On the elastic sonogram images, a shear wave velocity, shear modulus, or Young's modulus higher than that of the surrounding normal muscle was defined as enhanced stiffness, while values lower than the surrounding normal muscle were defined as decreased stiffness.

Correlations Between Ultrasound Features and Histopathological Findings

One physician with over 10 years of experience in ultrasound and 1 pathologist with more than 10 years of experience in diagnostic pathology compared the skeletal muscle biopsy tissue sections with their corresponding ultrasound-guided biopsy images. The HE-stained sections were assessed to determine whether muscle fibers were present, the extent of fibrosis, whether proliferating lymphocytes were distributed along the long axis of muscle fibers, and whether there was vascular proliferation, necrosis, or calcification.

Statistical Analysis

Statistical analyses were performed using SPSS version 26.0 (IBM, Armonk, NY, USA). Continuous variables that followed a normal distribution are presented as the mean ± standard deviation (SD), while non-normally distributed continuous variables are presented as the median (25th to 75th percentiles). The Kappa test was utilized to assess and compare the consistency between ultrasound features and pathological characteristics. A kappa value <0.4 indicates poor consistency, 0.4 ≤ kappa ≤0.75 indicates moderate consistency, and a kappa value >0.75 indicates good consistency. A P-value of <0.05 was considered statistically significant for 2-sided tests.

Results

Clinical Findings

The study cohort consisted of 35 patients (mean age, 63 years ±15 [SD], 17 men and 18 women). Among the 35 cases of muscle lymphoma, 3 (8.6%) were located in the upper limbs, 7 (20.0%) were located in the lower limbs, 16 (45.7%) were located in the trunk, and 9 (25.7%) were located in the head and neck region. A palpable mass was the most common chief complaint (88.6%) (Figures 2 and 3). Thirty-one (88.6%) patients presented with involvement of other tissues or organs besides muscle (Table 1).

Pathology

All patients underwent ultrasound-guided biopsy. Among them, 21 (60%) patients had skeletal muscle biopsies, 13 (37.1%) had lymph node biopsies, and 1 (2.9%) had a breast biopsy. The pathological subtypes were primarily diffuse large B-cell lymphoma (68.6%), followed by peripheral T-cell lymphoma (8.6%), marginal zone lymphoma (5.7%), anaplastic large cell lymphoma, anaplastic lymphoma kinase-positive large B-cell lymphoma, Epstein–Barr virus-positive diffuse large B-cell lymphoma, Burkitt lymphoma, small B-cell lymphoma, and mantle cell lymphoma, all of which also involved skeletal muscle in this group of cases (Table 2).

The histopathologic features of muscular lymphoma are summarized as follows: Lymphocytic proliferation was observed in all 21 (100%) tissue sections. Twelve (57.1%) cases showed normal muscle fibers, 5 (23.8%) cases exhibited substantial fibrosis, 3 (14.3%) cases had capillary proliferation, and 2 (9.5%) cases showed tissue necrosis.

Figure 1. A, Myofiber-like echoes within a lymphoma in the flexor carpi ulnaris muscle. Some of these echoes are continuous with surrounding normal muscle fibers (long arrows), while others show interruptions or absence of echoes (short arrows). **B**, A longitudinal ultrasound image of the flexor carpi ulnaris in a healthy individual. **C**, The cobblestone appearance (asterisk) of a lymphoma in the gluteus maximus. **D**, A transverse ultrasound image of the gluteus maximus in a healthy subject.

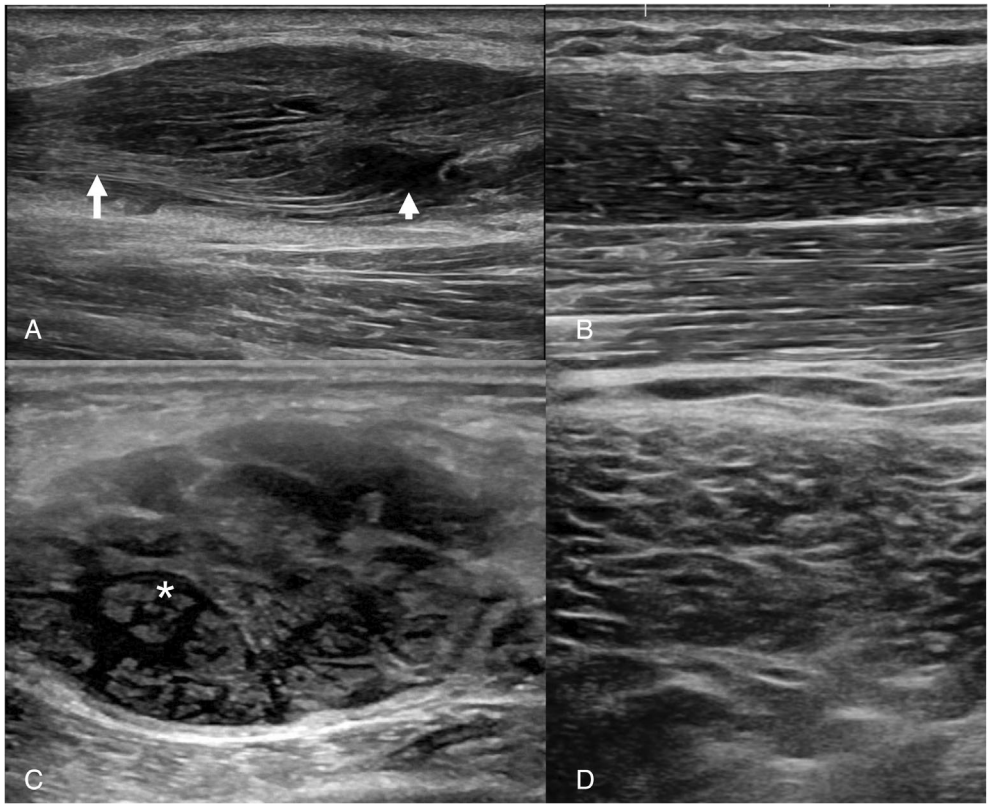

Figure 2. An elderly male patient presented with a palpable mass on his right leg. **A**, The patient's right lower leg was swollen (black arrow). **B**, Panoramic ultrasound imaging of the lateral aspect of the right lower leg revealed fusiform hypoechoic regions with a poorly defined margin within multiple skeletal muscles. The long axis of the lesions was consistent with the muscle fibers' long axis. **C**, The long-axis sonogram of the lesion showed hyperechoic muscle fiber-like structures within the hypoechoic region. **D**, The short-axis view showed a "cobblestone" appearance (white arrow). **E**, Power Doppler imaging revealed abundant blood flow signals within the lesion. **F**, Color-Doppler imaging showed transverse blood flow signals (asterisk) within the lesion, presenting a low-resistance arterial spectrum. **G**, A biopsy was taken under ultrasound guidance from the hypoechoic region. **H**, Histological examination of the biopsy site showed a large number of abnormally proliferating lymphocytes surrounding the muscle fibers (hematoxylin and eosin, ×10). **I**, Myofiber lysis is shown in the histology (hematoxylin and eosin, ×40). d, dermis; s, subcutaneous tissue; m, muscle; L, lesion.

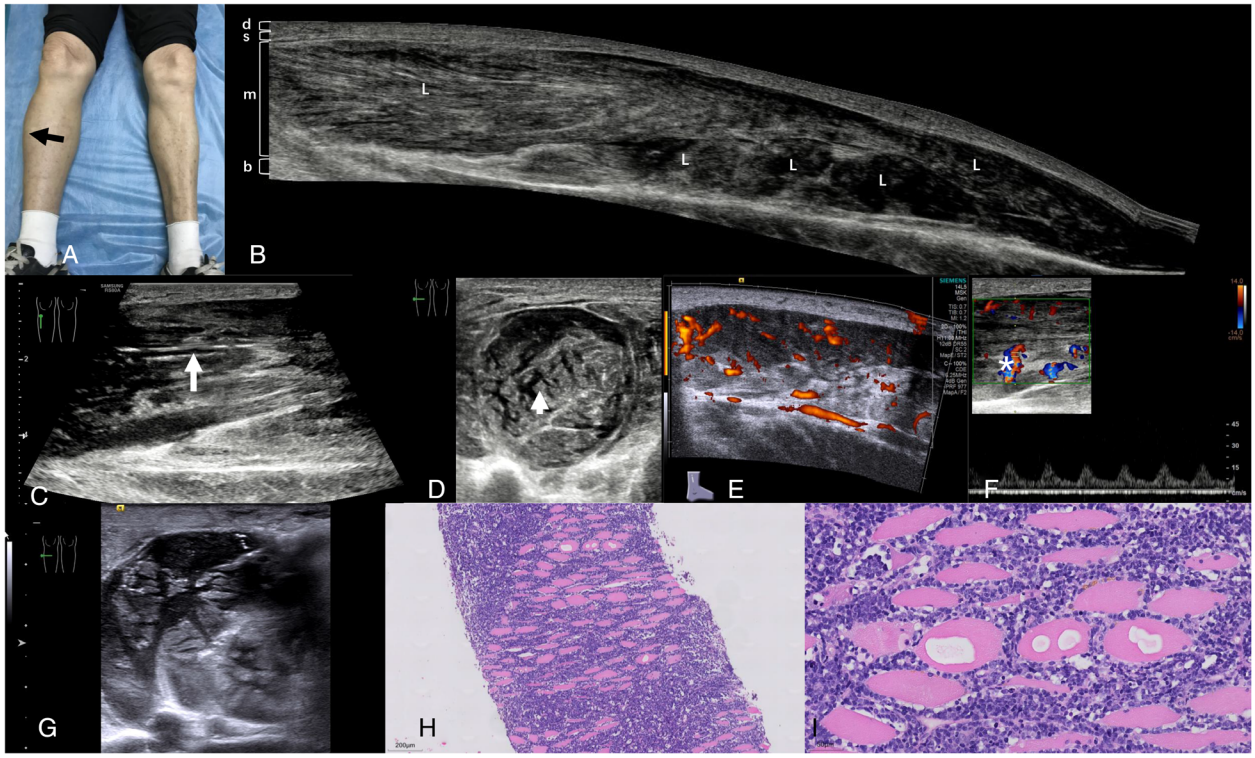

Multimodal Ultrasound Features

Gray-Scale Ultrasound

Of the 35 cases, 14 (40%) involved a single muscle and 21 (60%) involved multiple muscles. Among the 35 lesions, 19 (54.3%) exhibited fusiform morphology, 4 (11.4%) were quasi-circular, and 12 (34.3%) were irregular in shape. In 33 (94.3%) cases, there was extension of the tumor along the long axis of the muscle. All lesions had poorly defined margins. The epimysium showed continuity in 30 (85.7%) cases, whereas the lesion breached the epimysium and invaded the surrounding tissues in 5 (14.3%) cases. There was no strong echogenicity representing calcification in any of the cases. Eight (22.9%) patients presented with concurrent thickening of the dermis and subcutaneous soft tissues (Table 3).

In terms of the internal echotexture characteristics, residual myofiber-like echoes were observed in 25 (71.4%) cases (Figure 4) on the sonograms performed along the long axis of the lesion. In 18 (51.4%) cases, a "cobblestone" appearance was observed on the sonograms performed along the short axis of the lesion. These "cobblestone" pattern changes were either diffused throughout the central part of the lesion (Figure 2) or exhibited a focal distribution around the periphery of the lesion (Figure 5). Six (17.1%) patients had no muscle fiber echoes or "cobblestone" appearance within the lesion.

Figure 3. An elderly male patient presented with a palpable mass on the right neck. **A**, A bulge was visible on the patient's neck (arrow). **B**, A panoramic long-axis image of the sternocleidomastoid muscle showed heterogeneous hypoechoic areas within the muscle with an ill-defined margin and unclear muscular epimysium. **C**, A panoramic short-axis image of the lesion revealed a mix of hyperechoic and hypoechoic areas. **D**, Color-Doppler ultrasound revealed no blood flow signals in some muscle fiber regions and abundant blood flow signals in other regions. **E**, Contrast-enhanced ultrasound showed no enhancement in some areas. **F**, Accompanied by subcutaneous soft tissue edema and thickening, along with lymph node enlargement (asterisk). **G**, A biopsy was taken under ultrasound guidance from the heterogeneous hypoechoic area. **H**, Histological examination of the biopsy (hematoxylin and eosin, ×10). **I**, Short-axis region of muscle fibers shown in histology (hematoxylin and eosin, ×40). **J**, Necrotic area in muscle (hematoxylin and eosin, ×100). d, dermis; s, subcutaneous tissue; m, muscle; b, bone; L, lesion.

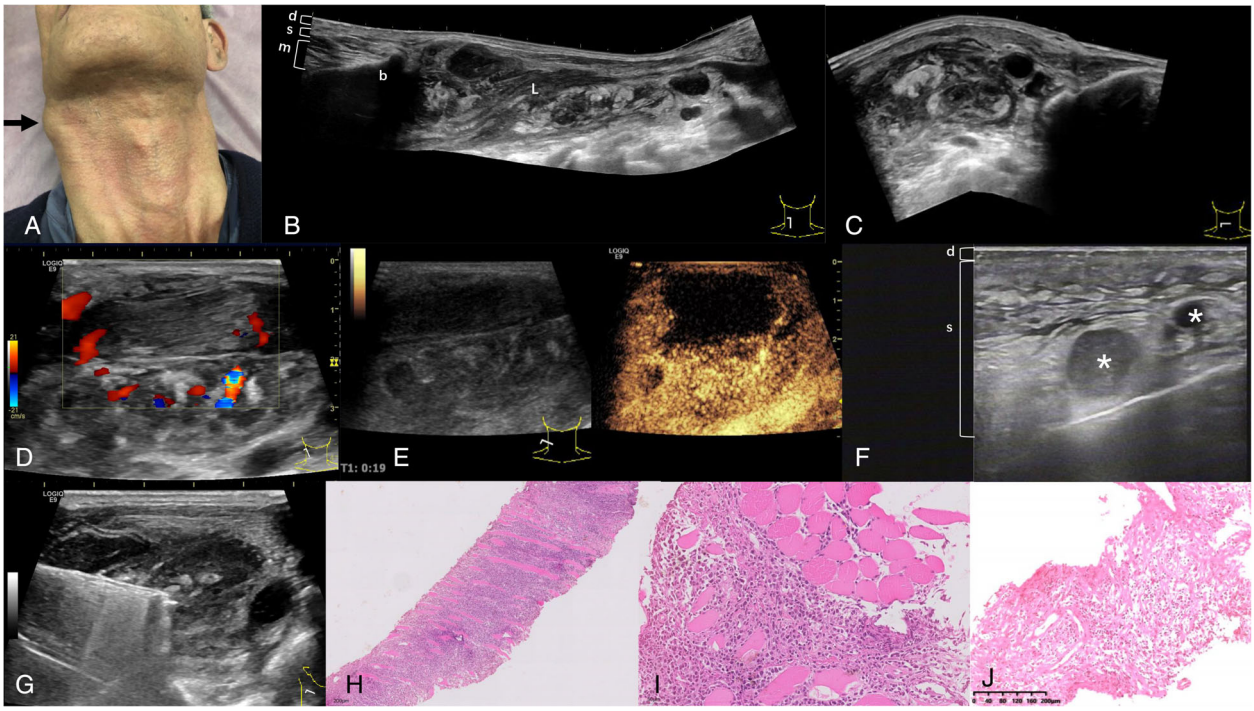

Color-Doppler Ultrasound

Color-Doppler sonograms were available for all 35 patients. These showed rich blood flow signals for 29 (82.9%) lesions, minimal blood flow signals for 6 (17.1%) lesions, and no blood flow signals for 2 (5.7%) lesions. Regions without blood flow signals on ultrasound were confirmed to have localized necrosis on histological sections (Figure 3). Ten (28.6%) cases showed intact transverse vessels perpendicular to the long axis of the muscle (Figures 2 and 4–7).

Contrast-Enhanced Ultrasound

Five (14.3%) patients underwent CEUS examination. Among them, 4 out of 5 (80%) cases showed synchronous strong enhancement comprising homogeneous enhancement in 2 (40%) cases (Figure 7) and inhomogeneous enhancement in 2 (40%) cases (Figure 8). These 4 cases also had rich blood flow signals in the color-Doppler sonogram. The remaining 1 case showed no enhancement within the lesion and displayed no blood flow signals on the color-Doppler sonogram (Figure 3).

Elastography

Four patients underwent elastography before chemotherapy. Elastography indicated enhanced stiffness in 4 patients (Figures 4 and 5). One patient underwent elastography after chemotherapy and had a lesion stiffness that was less than that of normal muscle (Figure 6) (Table 4).

Table 1. Clinical Information From the 35 Patients With Skeletal Muscle Lymphoma

	Number	Percentage (%)
Sex		
Female	17	48.6
Male	18	51.4
Site		
Head and neck	9	25.7
Trunk	16	45.7
Upper limbs	3	8.6
Lower limbs	7	20.0
Chief complaint		
Palpable mass	31	88.6
Pain	17	48.6
Weight loss	6	17.1
Fever	3	8.6
With other tissue or organ involved	34	97.1

Table 2. Histopathological Information from the 35 Patients with Lymphoma

	Number	Percentage (%)
Puncture site	35	100
Muscle	21	
Lymph node	13	
Breast	1	
Pathological type		
DLBCL	24	68.6
PTCL	3	8.6
MZL	2	5.7
ALCL	1	2.9
ALK + LBCL	1	2.9
EBV + DLBCL	1	2.9
BL	1	2.9
SBL	1	2.9
MCL	1	2.9

DLBCL, diffuse large B-cell lymphoma; PTCL, peripheral T-cell lymphoma; MZL, marginal zone lymphoma; ALCL, anaplastic large cell lymphoma; ALK + LBCL, ALK positive large B-cell lymphoma; BL, Burkitt lymphoma; SBL, small B-cell lymphoma; MCL, mantle cell lymphoma.

Correlations Between Multimodal Ultrasound Features and Histopathological Findings

Among the 21 patients who underwent skeletal muscle biopsy, ultrasound-guided biopsies at locations corresponding to myofiber-like echo areas revealed muscle fibers that still retained their normal structure upon histological examination. In these cases, a large number of abnormally proliferated lymphocytes were diffusely distributed around the muscle fibers (Figure 4). The ultrasound showed a "cobblestone" appearance, and histologically, these patients exhibited further abnormal lymphocyte proliferation, with some areas showing a complete absence of muscle fiber structures (Figures 2 and 5). The lesions with no myofiber-like echoes and a "cobblestone" appearance resembled hypoechoic mass-like appearance. Histologically, these lesions contained a large number of proliferating lymphocytes, with no visible muscle fibers.

Table 3. Imaging Findings of Muscular Lymphoma on Gray-Scale Ultrasound

	Number	Percentage (%)
Number		
Single	14	40.0
Multiple	21	60.0
Shape		
Fusiform	19	54.3
Quasi-circular	4	11.4
Irregular	12	34.3
Size		
<5 cm	22	62.9
5 ≤ d < 10 cm	6	17.1
≥10 cm	7	20
Along the long axis of the muscle		
Yes	33	94.3
No	2	5.7
Epimysium continuity		
Yes	30	85.7
No	5	14.3
Thickening of the skin and subcutaneous fat		
Yes	8	22.9
No	27	77.1
Internal architecture of the lesion		
Residual myofiber-like echoe	25	71.4
"Cobblestone" appearance	18	51.4
Mass like appearance	6	17.1

Kappa analysis showed that the ultrasound features that were significantly correlated with normal muscle fibers on histology were residual myofiber-like echoes (κ: 0.8, $P < 0.001$) and "cobblestone" appearance (κ: 0.521, $P < 0.017$). The presence of a mass-like appearance on the ultrasonogram was negatively correlated with histopathological normal muscle fibers (Table 5).

Two (5.7%) patients who showed no blood flow signals in color-Doppler sonograms underwent

Figure 4. A middle-aged patient presented with a palpable mass on the forearm. **A**, Gray-scale ultrasound revealed a fusiform hypoechoic region within the ulnar flexor carpi muscle, with a poorly defined margin. The long axis of the lesion was consistent with the muscle fibers' long axis, and hyperechoic striated structures were visible inside, resembling muscle fibers (white arrow) retaining continuity with the surrounding muscles. **B**, In the short-axis view of the lesion, dot-line hyperechoic patterns were observed within the hypoechoic area. **C**, Color Doppler imaging showed abundant blood flow signals within the lesion, along with traversing vessels perpendicular to the muscle's long axis (asterisk). **D**, Sequential scanning revealed 2 vessels branching from the ulnar artery, supplying the lesion. **E**, Elastography indicated that the lesion was stiffer than the surrounding area. **F**, Shear wave elastography demonstrated increased shear wave velocity within the lesion, averaging 4.7 m/s, while the normal muscle tissue had an average shear wave velocity of 1.5 m/s. **G**, A biopsy was taken under ultrasound guidance from the hypoechoic region. **H**, Histological examination of the biopsy site showed a large number of abnormally proliferating lymphocytes surrounding the muscle fibers, with destruction of the muscle fiber structure in some areas (short arrow), while skeletal muscle structure was still observable in other areas (long arrow) (hematoxylin and eosin, ×10). **I**, Long-axis region of muscle fibers shown in histology (hematoxylin and eosin, ×40). **J**, Short-axis region of muscle fibers shown in histology (hematoxylin and eosin, ×40). d, dermis; s, subcutaneous tissue; m, muscle; L, lesion.

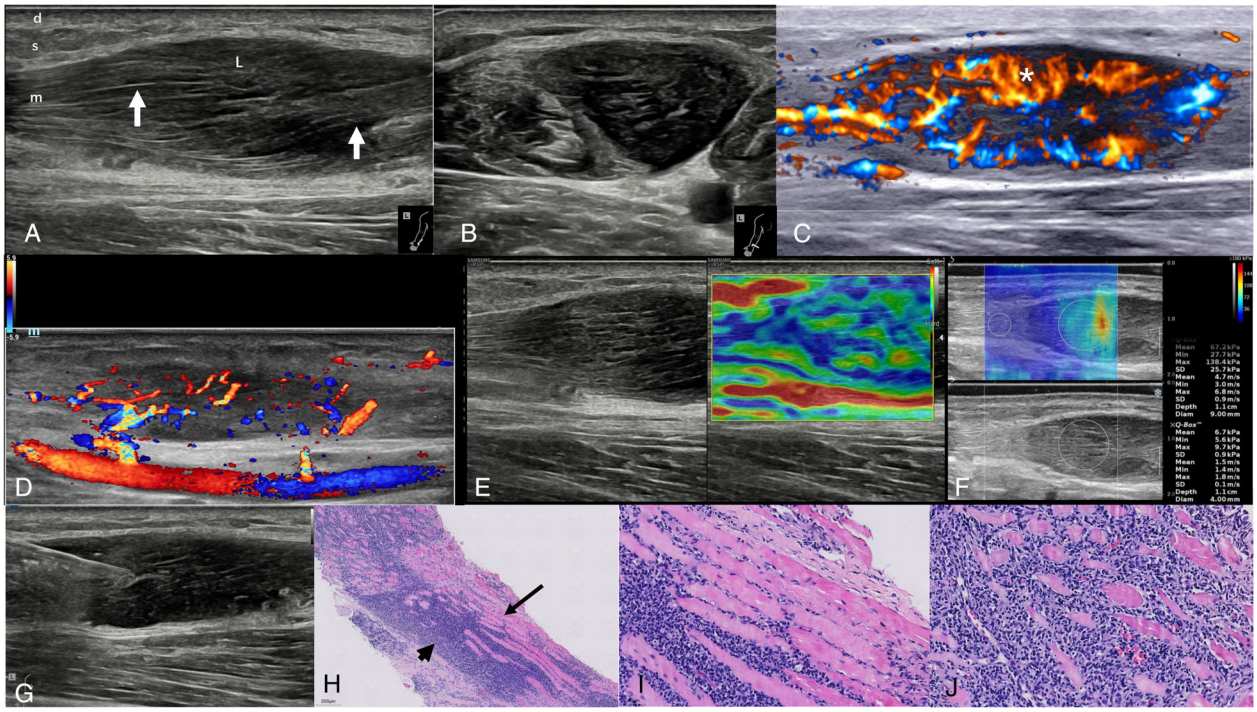

further CEUS, which also showed no enhancement. The non-enhanced area was localized necrotic tissue, which was confirmed by ultrasound-guided biopsy. In our review of color-Doppler flow images and ultrasound-guided biopsy images, we found that the biopsy site did not always match the area shown on the Doppler image. Therefore, it was challenging to assess the correlation of vascular proliferation seen in Doppler images with the histopathological findings.

Four patients underwent elastography before chemotherapy and had tissue samples taken. Elastography indicated enhanced stiffness, but histology did not show substantial fibrosis or necrosis. One patient underwent post-chemotherapy elastography that showed decreased stiffness. However, due to ethical considerations, the post-treatment tissue was not biopsied, making it difficult to explore the pathological mechanisms behind the decreased stiffness.

As biopsy specimens generally do not include the epimysium, subcutaneous tissue, or areas suspected of calcification as seen on ultrasound, the morphological features related to these aspects were not discussed here.

Discussion

We conducted a retrospective analysis of ultrasound findings in patients who were diagnosed with muscle

Figure 5. An elderly male presented with a neck mass. **A**, Panoramic ultrasound imaging of the lesion showed that the main body of the lesion was located within the sternocleidomastoid muscle, with a poorly defined margin. The long axis of the lesion was consistent with the muscle fibers' long axis. **B**, The long-axis sonogram revealed muscle fiber-like hyperechoic (white long arrow) regions at the edge of the lesion. **C**, The short-axis sonogram showed a "cobblestone" appearance (white short arrow) around the lesion. **D**, Elastography indicated that the lesion was harder compared to the surrounding normal tissue. **E**, Shear wave elastography revealed an increased shear wave velocity inside the lesion, averaging 2.63 m/s, while the surrounding normal muscle tissue had an average shear wave velocity of 1.69 m/s. **F**, Color-Doppler ultrasound displayed abundant blood flow signals within the lesion, including transverse vessels (asterisk) perpendicular to the muscle's long axis. **G**, A biopsy was taken under ultrasound guidance from the hypoechoic region. **H**, Histological examination of the biopsy site showed that only a small amount of muscle fiber structure remained on one side of the lesion, while most areas were devoid of normal muscle fibers (hematoxylin and eosin, ×10). **I**, The center of the lesion consisted of abnormally proliferating lymphocytes with no muscle fibers (hematoxylin and eosin, ×40). **J**, Muscle fibers were visible in the surrounding areas of the lesion (hematoxylin and eosin, ×40). d, dermis; s, subcutaneous tissue; m, muscle; L, lesion.

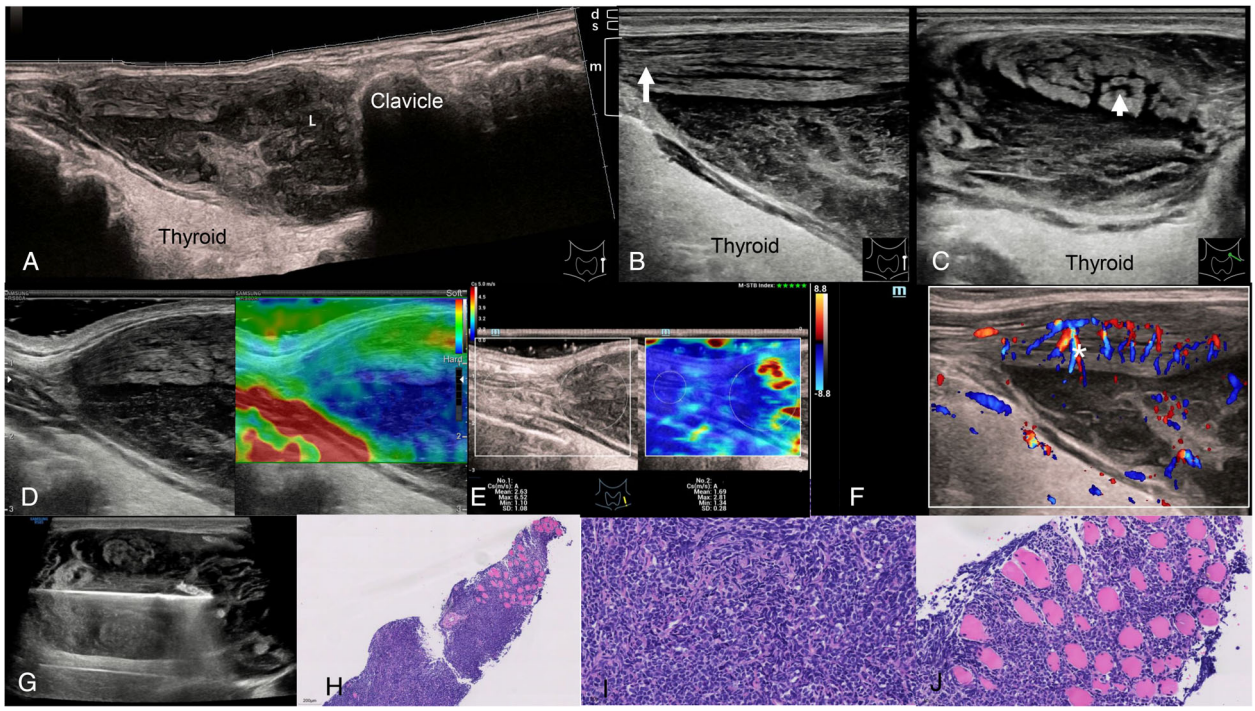

lymphoma at our hospital over a 10-year period to explore the ultrasound features of skeletal muscle lymphoma and investigate the relationship between these features and the underlying pathological mechanisms.

It was reported that 75% of muscle lymphoma lesions can be visualized as fusiform lesions along the long axis of the skeletal muscle on magnetic resonance imaging (MRI).[5,6] In this study using ultrasonography, we found that 51.4% of lesions were fusiform and 91.9% had the same long axis as the muscle. These findings may be related to lymphocytes extending along the long axis of the muscle, that is, along the direction of neurovascular bundles.[7]

High-frequency ultrasound can display fine structures within muscles[8]; therefore, recent case reports have stated that lymphoma lesions within muscles can be visualized by high-frequency ultrasound as coarsened fibroadipose septa echoes, continuous with surrounding unaffected muscle fibers.[9] In this study, residual myofiber-like echoes were observed in 25 cases (71.4%), which would serve as an indicator to diagnose skeletal muscle lymphoma. It is noteworthy that all these cases showed hypoechoic features, and appropriately increasing the gain during scanning may further increase the detection rate of residual myofiber-like echoes.

The present study also revealed another striking ultrasound feature that has not been reported in

Figure 6. An elderly male presented with a mass on his back before and after chemotherapy. **A**, The initial panoramic ultrasound imaging showed that the main body of the lesion was located between the latissimus dorsi and external oblique muscles, with a poorly defined margin. The long axis of the lesion was consistent with the muscle fibers' long axis. **B**, The longitudinal sonogram revealed a small amount of muscle fiber-like hyperechoic areas (white long arrow) within the lesion. **C**, The short-axis sonogram showed a "cobblestone" appearance (white short arrow) around the lesion. **D**, Color-Doppler ultrasound displayed abundant blood flow signals within the lesion, including transverse vessels (asterisk) perpendicular to the muscle's long axis. **E**, Histological sections showed abnormally proliferating lymphocytes (hematoxylin and eosin, ×10). **F**, After chemotherapy, panoramic ultrasound imaging revealed a significant reduction in the size of the lesion. **G**, The long-axis sonogram after chemotherapy showed muscle fiber-like hyperechoic areas (black long arrow) within the lesion. **H**, The short-axis sonogram after chemotherapy displayed a "cobblestone" appearance (black short arrow) around the lesion. **I**, Color-Doppler ultrasound after chemotherapy revealed no blood flow signals within the lesion. **J**, Elastography after chemotherapy indicated that the lesion was softer compared to its surrounding tissue. **K**, Shear wave elastography showed a reduced shear wave velocity inside the lesion, averaging 1.3 m/s, while the surrounding normal echogenic muscle tissue had an average shear wave velocity of 1.5 m/s. d, dermis; s, subcutaneous tissue; m, muscle; L, lesion.

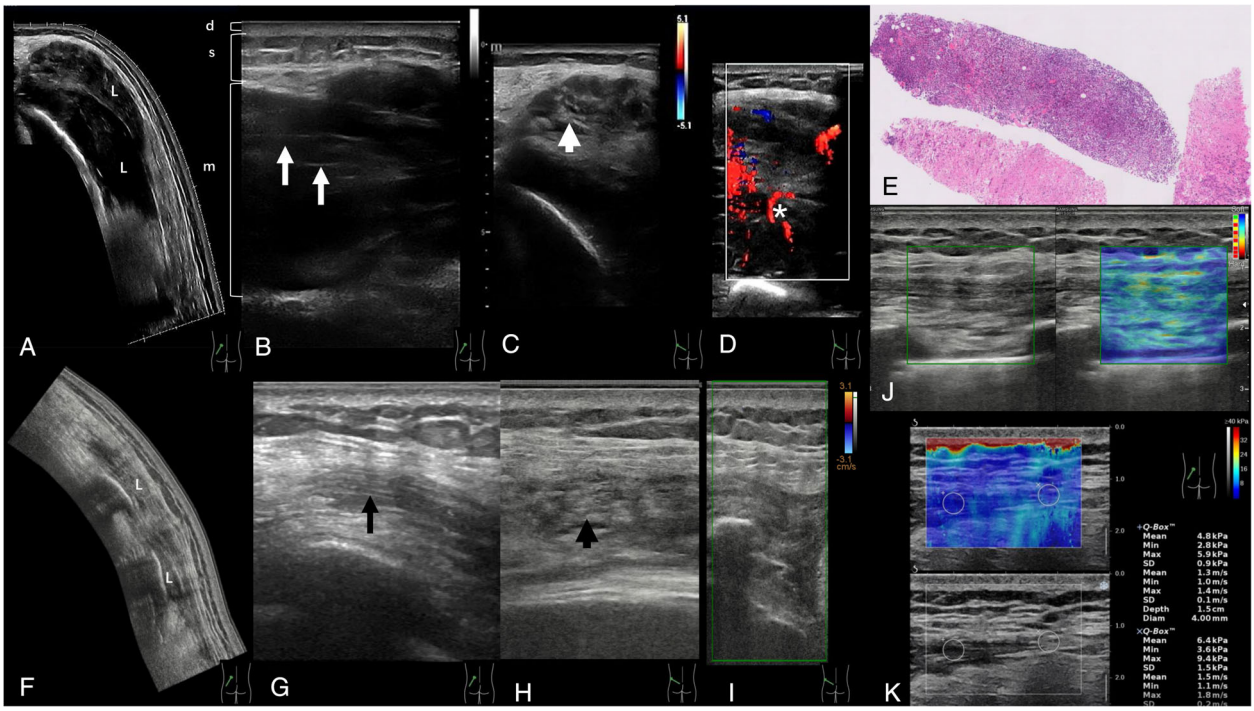

previous studies. On retrospective analysis of the short-axis sonograms of lesions, we found that 51.4% of patients had hypoechoic areas interspersed with hyperechoic areas within the lesions, and that the hyperechoic areas were segmented into multiple small patches. The histological manifestation at this stage is the diffuse proliferation of lymphocytes in the muscle interstitium, distributed around muscle fiber gaps, with normal or partially dissolved muscle fiber structures. On the basis of this pathological status, we believe that the multiple small patchy hyperechoic areas observed in the sonograms reflect relatively normal muscle fibers surrounded by hypoechoic areas representing abnormally proliferating lymphocytes. Due to the dense arrangement of lymphocytes, ultrasound cannot be reflected at the tissue interfaces, resulting in hypoechoic areas. These areas appeared as segmented small blocks of hyperechoic structures on ultrasound, which we interpreted as muscle fibers surrounded by lymphocytes. This characteristic image finding can appear in the center or periphery of the lesion and represents the main growth pattern of lymphoma in the muscle interstitium, with muscle fibers at a stage of incomplete destruction.

When the lesions were evaluated on color-Doppler ultrasound, 28.6% exhibited blood flow signals

Table 4. Imaging Findings of Muscular Lymphoma on Color-Doppler, Contrast-Enhanced Ultrasound, and Elastography

	Number	Percentage (%)
Color-Doppler ultrasound		
Increased vascularity	28	80.0
Minimal vascularity	5	14.3
No vascularity	2	5.7
Intact traversing vessels		
Yes	10	28.6
No	25	71.4
Contrast enhanced ultrasound		
Homogeneous enhancement	2	40
Inhomogeneous enhancement	2	40
No enhancement	1	20
Elastography		
Enhanced stiffness	4	80
Decreases stiffness	1	20

perpendicular to the long axis of the muscle. This phenomenon was also mentioned in an analysis of the MRI features of 20 cases of muscle lymphoma, in which 17 (85%) patients had complete transverse vascular flow within the affected muscles.[5] As Doppler signal assessment of the blood flow of lesions depends on the operator's technique and the instrument settings, the detection rate of transverse vessels may increase as ultrasound physicians become more familiar with this phenomenon. We speculate that the perpendicular blood flow signal observed during ultrasound scanning may be due to the expansion of pre-existing nutrient vessels within the muscle. Since biopsies are generally conducted under ultrasound guidance to prevent injury to blood vessels and nerves, assessing the correlation

Figure 7. An elderly male presented with a palpable mass in the left inguinal region. **A**, The panoramic view of the iliopsoas muscle in the longitudinal direction revealed a hypoechoic area within the muscle with an ill-defined margin. The long axis of the lesion was consistent with the muscle fibers' long axis. **B**, Low-frequency ultrasound showed that the lesion invaded outward, reaching the periphery of the iliac vessels, and the epimysium was not clearly visible. **C**, High-frequency ultrasound revealed muscle fiber-like hyperechoic areas (white long arrow) within the lesion's long axis. **D**, On the short-axis view of the lesion under high-frequency ultrasound, alternating hyperechoic and hypoechoic areas were observed. **E**, Color-Doppler ultrasound of the lesion's long axis displayed abundant blood flow signals. **F**, Color-Doppler ultrasound of the lesion's short axis revealed transverse vessels (asterisk) perpendicular to the muscle's long axis. **G**, Contrast-enhanced ultrasound demonstrated a hyperenhancement pattern. **H**, A biopsy was taken under ultrasound guidance from within the hypoechoic region. **I**, Histological examination of the biopsy site showed the disappearance of normal muscle fibers and the presence of numerous neovascularizations (arrows) within the lesion (hematoxylin and eosin, ×40). **J**, The neovascularizations in the stroma varied in diameter (arrows) (hematoxylin and eosin, ×40). d, dermis; s, subcutaneous tissue; m, muscle; L, lesion.

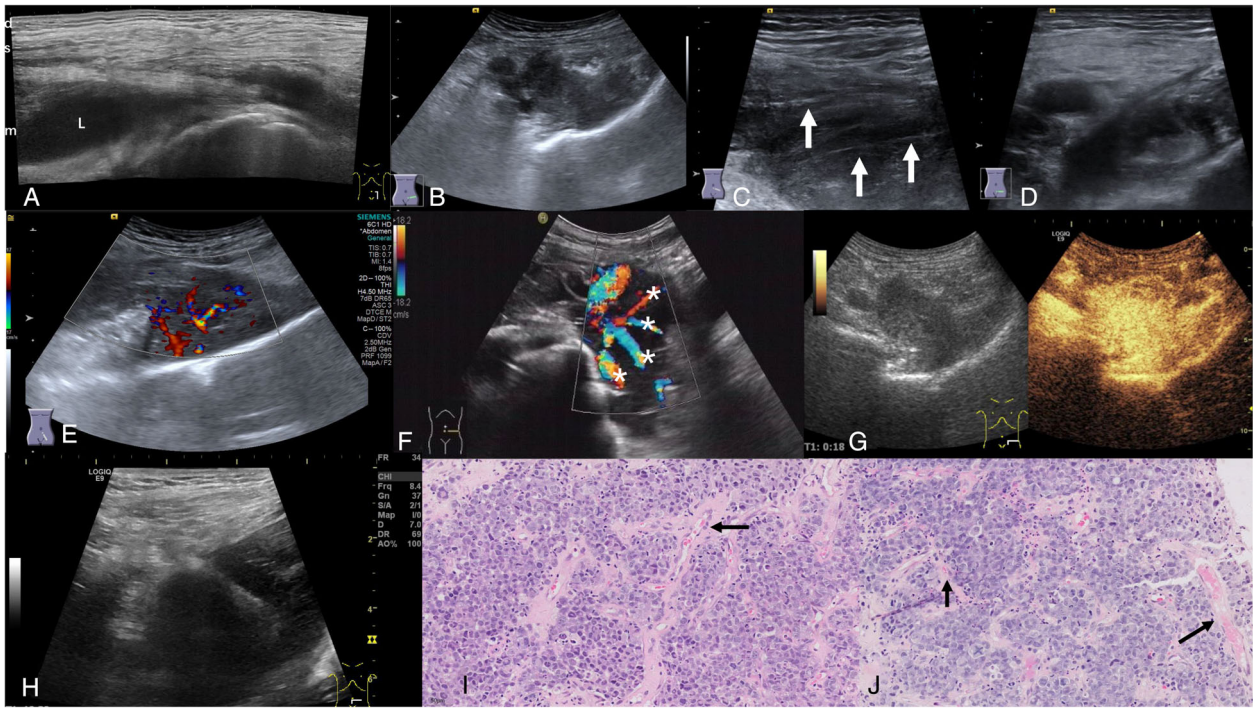

Figure 8. An elderly female presented with an abdominal mass and pain. **A**, The panoramic view of the lesion in the longitudinal direction of the rectus abdominis revealed an inhomogeneous fusiform hypoechoic region within the rectus abdominis, with ill-defined boundaries. The long axis of the lesion was consistent with the muscle fibers' long axis. **B**, The long-axis sonogram of the lesion showed muscle fiber-like hyperechoic areas (white long arrow) within the hypoechoic region. **C**, On the short-axis view, an interweaving pattern of hyperechoic and hypoechoic areas (white short arrow) was observed. **D**, Color-Doppler ultrasound revealed slightly abundant blood flow signals within the lesion. **E**, Spectral Doppler ultrasound demonstrated low-resistance arterial blood supply within the lesion. **F**, Contrast-enhanced ultrasound showed an iso-enhancement pattern of the lesion. **G**, A biopsy was taken under ultrasound guidance from the hypoechoic region. **H**, Histological examination of the biopsy site showed a large number of abnormally proliferating lymphocytes surrounding the muscle fibers. In some areas, the muscle fiber structure was damaged (short arrow), while in other areas, the skeletal muscle structure was still visible (long arrow) (hematoxylin and eosin, ×10). **I**, Short-axis view of muscle fibers in the histology (hematoxylin and eosin, ×40). **J**, Long-axis view of muscle fibers in the histology (hematoxylin and eosin, ×40). d, dermis; s, subcutaneous tissue; m, muscle; L, lesion.

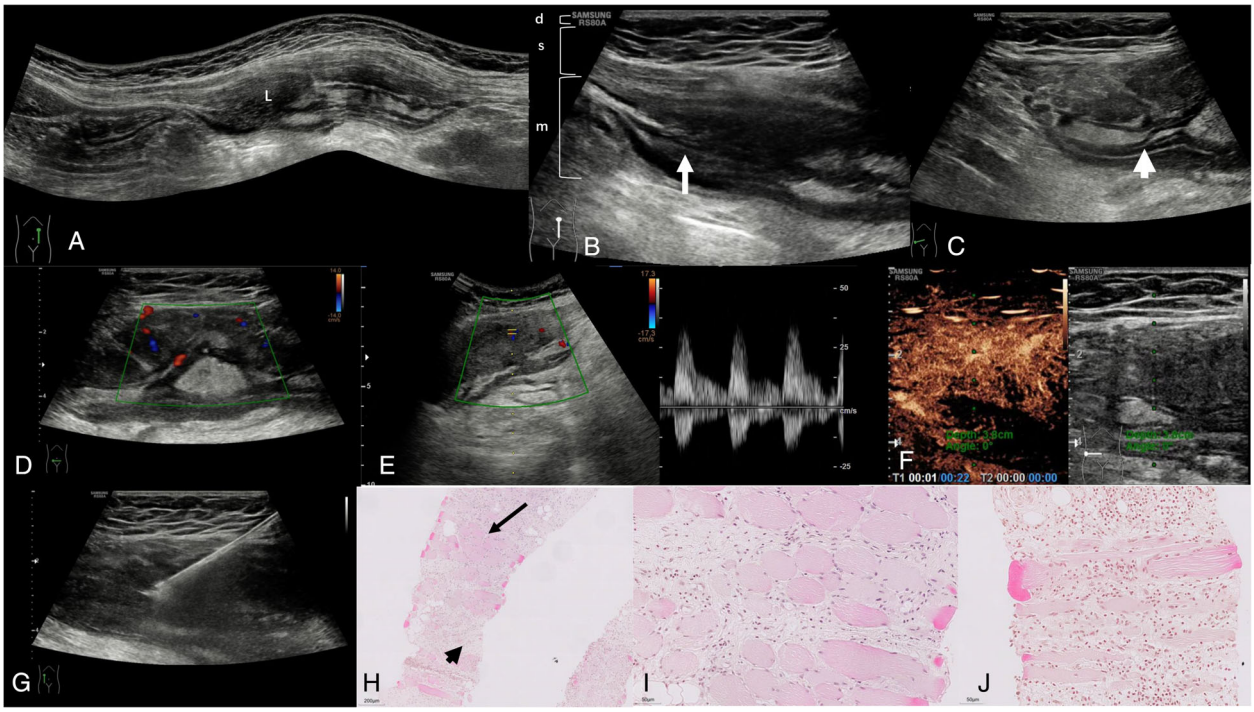

between the vascular proliferation observed in Doppler images and the histopathological findings proved to be a formidable challenge.

Currently, there are no reports on the CEUS and elastography features of muscle lymphoma. On contrast-enhanced MRI, muscle lymphoma may show peripheral thick band-like enhancement and deep fascial enhancement, homogeneous enhancement, or heterogeneous enhancement, with areas of necrosis within the lesion.[6,10] In our study, the enhancement characteristics of lesions showing homogeneous enhancement, heterogeneous enhancement, or no enhancement were observed. However, due to the smaller area observed in CEUS compared to contrast-enhanced MRI, peripheral thick band-like enhancement and deep fascial enhancement were not observed. A larger sample size may be needed for prospective studies. Five patients underwent pressure or shear wave elastography, with the 4 patients who were evaluated before chemotherapy showing increased tissue stiffness within the lesions compared with surrounding muscle tissue, whereas the patient who was evaluated after chemotherapy showed decreased tissue hardness. The increase in tissue hardness may be related to increased fascial compartment pressure caused by the dissolution of muscle fibers.[11,12] This suggests that elastography may assist in diagnosing local muscle pressure increases caused by lymphoma; however, because of the small number of cases examined, the value of CEUS and elastography in the diagnosis of lymphoma remains unclear.

Table 5. Consistency of Histopathological Changes and Ultrasonic Features in the 21 Patients With Pathological Section of Skeletal Muscle Puncture Tissue

	Histopathological Changes		Kappa	*P*
Ultrasonic Features	**Muscle fiber**	**Without muscle fiber**		
Residual myofiber-like echoes			0.800	<.001
Yes	7	0		
No	2	12		
"Cobblestone" appearance			0.521	.017
Yes	7	3		
No	2	9		
Mass like appearance			−0.615	.001
Yes	3	12		
No	6	0		

Combining the ultrasound and histological characteristics of muscle lymphoma from different cases, we speculate that in the early stage of muscle lymphoma, lymphocytes proliferate diffusely in the muscle interstitium, preserving the normal muscle fiber structure. Ultrasound sonograms may show a blurred hypoechoic area with preserved normal muscle fiber structure, and myofiber-like echoes continuous with surrounding normal muscle fibers can be seen after gain adjustment. As lymphocytes further proliferate, some muscle fibers are destroyed and dissolve, resulting in hypoechoic areas surrounding small patchy hyperechoic areas along the short axis that resemble the "cobblestone" appearance that can occur in the center or periphery of the lesion. In the later stage of the disease, the muscle fibers completely dissolve, and ultrasound images show mass-like appearance, making it difficult to distinguish the muscle structure.

During the diagnostic process of muscle lymphoma, several differential diagnoses should be considered. For example, myopathies and myositis may also present with residual myofiber-like echoes on ultrasound, along with edema in the dermis and subcutaneous tissue. However, unlike lymphomas, which typically appear as hypoechoic masses, myopathies and myositis usually demonstrate overall increased echogenicity.[13] In addition, when a "cobblestone" appearance is observed within a lesion, it should be differentiated from lymphatic vessel dilatation in soft tissue. In the subcutaneous fat layer, a "cobblestone" pattern is commonly associated with massive dilation and distension of lymphovascular branches, representing the hypoechoic component of this distinctive sonographic pattern.[14] In contrast, in skeletal muscle lymphoma, muscle fibers have a specific orientation, and the "cobblestone" appearance is typically observed only in the short axis of the muscle, unlike subcutaneous edema, where the pattern can be seen in all directions. When a mass-like appearance is present in muscle lymphoma, it is important to distinguish it from sarcoma, rhabdomyosarcoma, and osteosarcoma. Lymphoma is more likely to be associated with enlargement of regional lymph nodes and involvement of multiple organs. When differentiation is difficult, further biopsy is required. We believe that the diagnosis of muscle lymphoma can be facilitated by appropriately adjusting the gray-scale gain to detect residual internal muscle fibers (which may present as a "cobblestone" appearance in the short axis) and by performing dynamic scanning to identify transverse vessels that run perpendicular to the direction of muscle fibers and may be associated with involvement of other tissues or organs. Additionally, Doppler ultrasound and CEUS can help identify necrotic areas within lesions, thereby helping to avoid biopsying non-viable tissue.

The limitations of the present study are the retrospective design and the fact that the detection rates of ultrasound features may have been subjectively biased because of the limited understanding of the disease by the operating physicians. The retained color-Doppler images were single-frame rather than dynamic images and were typically focused only on areas that the operator considered most relevant at the time. As a result, it was difficult to reassess and refine the vascular details of the internal structure and borders of the tumor,

which are crucial for accurate tumor diagnosis. Additionally, the imaging features of new technologies such as CEUS and elastography remain unclear, particularly the lack of analysis of the vascular phases of CEUS. These features require investigation in further prospective studies. In our study, only 1 patient underwent follow-up ultrasound after treatment. We observed that the cobblestone appearance persisted post-treatment, although the extent of this appearance was reduced compared to pre-treatment. We speculate that post-treatment, fibrosis may have occurred within the interstitium of the skeletal muscle, replacing the previously proliferated lymphoid cells. Meanwhile, the preserved skeletal muscle fibers might have contributed to the continued appearance of the cobblestone pattern. However, due to ethical considerations, a post-treatment biopsy could not be performed, so this hypothesis remains unconfirmed.

Conclusion

Skeletal muscle lymphoma typically presents as a fusiform hypoechoic area with blurred borders along the long axis of muscle fibers on ultrasound images. Gray-scale sonogram may reveal residual myofiber-like echoes or "cobblestone" appearance. Additionally, there may be rich blood flow signals within the lesion, along with transverse vessels traversing perpendicular to the muscle fibers. In cases showing a combination of such features, a diagnosis of lymphoma should be strongly suspected.

Data Availability Statement

The data that support the findings of this study are available on request from the corresponding author. The data are not publicly available due to privacy or ethical restrictions.

References

1. Zucca E, Cavalli F. Extranodal lymphomas. *Ann Oncol* 2000; 11: 219–222.
2. Komatsuda M, Nagao T, Arimori S. An autopsy case of malignant lymphoma associated with remarkable infiltration in skeletal muscles (author's transl). *Rinsho Ketsueki* 1981; 22:891–895.
3. Lee VS, Martinez S, Coleman RE. Primary muscle lymphoma: clinical and imaging findings. *Radiology* 1997; 203:237–244.
4. Hongsakul K, Laohawiriyakamol T, Kayasut K. A rare case of primary muscular non-Hodgkin's lymphoma and a review of how imaging can assist in its diagnosis. *Singapore Med J* 2013; 54:e179–e182.
5. Chun CW, Jee WH, Park HJ, et al. MRI features of skeletal muscle lymphoma. *AJR Am J Roentgenol* 2010; 195:1355–1360.
6. Suresh S, Saifuddin A, O'Donnell P. Lymphoma presenting as a musculoskeletal soft tissue mass: MRI findings in 24 cases. *Eur Radiol* 2008; 18:2628–2634.
7. Navarro SM, Matcuk GR, Patel DB, et al. Musculoskeletal imaging findings of hematologic malignancies. *Radiographics* 2017; 37: 881–900.
8. Holsbeeck VM, Soliman S, Kerkhove FV, Craig J. Advanced musculoskeletal ultrasound techniques: what are the applications? *Am J Roentgenol* 2021; 216:436–445.
9. Gao S, Shu H, Yang H. Imaging features of skeletal muscle lymphoma: a case report and literature review. *BMC Med Imaging* 2021; 21:136.
10. Lim CY, Ong KO. Imaging of musculoskeletal lymphoma. *Cancer Imaging* 2013; 13:448–457.
11. Flowers CR, Sinha R, Vose JM. Improving outcomes for patients with diffuse large B-cell lymphoma. *CA Cancer J Clin* 2010; 60:393–408.
12. Masaoka S, Fu T. Malignant lymphoma in skeletal muscle with rhabdomyolysis: a report of two cases. *J Orthop Sci* 2002; 7: 688–693.
13. Ricci V, Ricci C, Cocco G, et al. From histology to sonography in skin and superficial tissue disorders: EURO-MUSCULUS/USPRM* approach. *Pathol Res Pract* 2022; 237:154003.
14. Albayda J, van Alfen N. Diagnostic value of muscle ultrasound for myopathies and myositis. *Curr Rheumatol Rep* 2020; 22:82.